Hydrogen Interaction in Fe Mn Al Alloys

U. BERNABAI and R. TORELLA - Dip ICMMPM Università "La Sapienza" - Roma

Abstract

Two Fe Mn Al steels, the one with austenite-ferrite structure (44% alfa-phase) and the other near fully austenitic structure (0.5% alfa-phase) and the AISI 304 stainless steel as reference, were submitted to thermal analysis after cathodic charging of hydrogen at a constant current density (8 mA/cm^2) for different times (100-400 min).

The emission diagrams of hydrogen for the three alloys have been considered at the light of the modern trapping theory.

Fe Mn Al steel with duplex structure out-degased a hydrogen bigger quantity than fully austenitic alloy.

In fact the austenitic structure with the presence of interstitial Carbon limits hydrogen apparent solubility.

Riassunto

Sono stati analizzati, mediante la tecnica dell'estrazione a caldo dell'idrogeno, a seguito di caricamento catodico (8 mA/cm^2) condotto per tempi variabili da 100 a 400 min, due acciai Fe Mn Al, il primo con struttura duplex austeno-ferritica (44% ferrite), l'altro con struttura pienamente austenitica (0.5% ferrite). I risultati sono stati confrontati con quello relativo all'acciaio inox ATSI 304, considerato come riferimento. I diagrammi di emissione dell'idrogeno sono stati interpretati secondo la moderna teoria dell'intrappolamento. La quantità di idrogeno estratto è risultata maggiore per l'acciaio Fe Mn Al con struttura duplex, rispetto all'acciaio con struttura pienamente austenitica, in quanto la presenza di C interstiziale in quest'ultima ne limita la solubilità apparente dell'idrogeno.

Introduction

The Mn-Al steel, generally named "poor man stainless steels" or Fe Mn Al alloys were born in order to have at one's austenitic or austenitic-ferritic cheaper steels with a good compromise for mechanical properties and resistance to corrosion in wet and hot environment. These steels, with nickel replaced by manganese and chromium replaced by aluminium, offer an interesting possibility of developing as substitutes of conventional stainless steesls [1-3].

Little is known about the interaction of these alloys with hydrogen. Recently a study on steels with austenitic-ferritic structure (90/10) and their susceptibility to hydrogen damage was referred (4).

According Perng and coworkers the cracking rate was basically controlled by hydrogen transport through the ferrite grains and, to control the hydrogen embrittlement, it's necessary to reduce the content of ferrite.

In general the reason of the brittle behaviour of ferritic structure is the much higher diffusivity and much lower solubility of the hydrogen [5-6].

The purpose of this work is to compare the thermal analysis of hydrogen charged Fe Mn Al alloys with a fully austenitic microstructure and with an austenitic-ferrite dual phase structure respect to that of conventional stainless steel AISI 304.

Thermal analysis method takes from the assumption that the escaping reaction of hydrogen from a trap site is a thermally activated process.

If E_{aT} is considered the activation energy of hydrogen to be released from a trap site and assuming that this energy is higher than that of the intercritical diffusion of hydrogen in b.c.c. iron, it's possible to write, for the hydrogen evolution rate from a trapping site, the following expression:

$$\frac{dX_\tau}{dt} = Ac\ (1-X_\tau)\exp\left(\frac{-E_aT}{RT}\right)$$

where X_τ is the fraction of the amount of hydrogen evolved from a trapping site, T is the absolute temperature, R is the universal gas constant, and A_c is a constant, respectively.

Heating with a uniform rate the hydrogen-charged specimen, the hydrogen evolution rate increases because of the rapid increase of the exponential term.

The evolution rate peak of hydrogen is formed at a certain temperature related to the trap activation energy of each trap. The amount of hydrogen trapped at each trap site can be calculated from the area of evolution rate peak [7].

Experimental procedure

Two FeMnAl alloys were used in this study, considering the AISI 304 Stainless Steel as a model steel.

The Alloy A with austenitic-ferritic structure with 44% of alfa phase (Fig. 1); the Alloy B with austenitic structure with 0.5% of alfa phase (Fig. 2).

The chemical analysis is shown in Tab. 1.

The alloys were produced from pure elements in an induction furnace under argon. After being smelted, the ingots were hot rolled into plates.

Rolling was started after homogenizing for one hour at 1050°C, finishing at about 900°C. The plates were treated again for 1 hour at 1050°C and then water quenched.

The specimens, with a cylinder shape (D = 6 mm, h = 20 mm) were surface finished.

TABLE 1 - Chemical compositions of materials

	C	Mn	Al	Fe	Cr	Ni
Alloy A	0.095	30.5	8.1	rest	/	/
Alloy B	0.95	23.3	7.4	rest	/	/
AISI 304	0.06	1.8	/	rest	18.5	9.5

with wet SiC paper n. 600, then rinsed in alcohol in ultrasonic apparatus.

Cathodic charging was performed at room temperature in a 0.1 N sulphuric acid solution, by the apparatus shown in Fig. 3.

The galvanostatic control of current density was 8 mA/cm^2 obtained with AMEL 551.

The charging time was varied from 100 min to 400 min. No external stress was applied during cathodic charging.

The cathodically charged specimen was cleaned by alcohol and dried, then the thermal analysis was curried out after 20 min break, by the furnace LECO HW200.

The detection method of the analysis furnace is based on cell that has ability to detect the difference in the thermal conductivity of gases.

The specimen was heated without a uniform rate, but with a settled trend presents in Tab. 2. This settled trend was established considering the traps classification as a function of trap activation temperature [8].

The detection apparatus printed the results showing a diagram of degased hydrogen from steel, measured in ml/100 g, as a function of temperature.

TABLE 2 - Function Time Temperature of Thermal Analysis

	TEMPERATURE (°C)	TIME (s)	RATE (°C/min)
Range A	50-400	300	200
Range B	400-600	300	200
Range C	600-800	600	200

Results

The thermal analysis of a hydrogenated specimen gives the partial quantities of hydrogen out-gased during the three temperature ranges which characterize the whole emission.

The emission diagrams (Fig. 4) related to the steel A, with duplex structure (44% of ferrite) and 0.095% of Carbon have two rather evident peaks, in corrispondence with the high maximum temperature of the first two ranges of analysis (50°C-400°C and 400°C-600°C), while during the third range (600°C-800°C), the hydrogen emission follows the trend of temperature approximately, increasing slowly during the heating and maintining the same costant value during the stationary phase.

The first peak of emission attains higher values than the second one and this difference grows with increase of charging time.

Also the emission diagrams (Fig. 5) of the steel B, with a mostly austenitic structure (0.5 of ferrite) and 0.95% of Carbon show two peaks that attain their maximum in correspondance of the final temperature of the first two ranges of thermal analysis. The emission of hydrogen during the third range, respect to the steel A, presents a slope slightly increasing even with a constant temperature.

The AISI 304 steel presents three peaks of out-gased hydrogen, each placed in a different temperature range.

The first peak results more evident, not extended in time for the limited quantity of escaped hydrogen from weak traps.

The second peak is more extended in time and it has a lower height compared with first one.

The third peak is highest then the former ones and it decreases slowly untill the end of the thermal analysis, giving the highest values of the quantity of out-degased hydrogen (Fig. 6).

Considering the diagrams of emission which show the partial and total quantities of hydrogen from the specimens as a function of charging time, it is possible to conclude as follows:

— The Mn-Al steel with duplex structure, signed "alloy A" shows a slowly increasing trend of the total quantity of hydrogen out-gased (Fig. 7) while the diagrams corresponding to the partially quantity out-gased during the different ranges offer different slopes. In particular it's possible to see an opposed trend of the diagrams related to the ranges one and three, while the range two presents a trend approximately constant with lower values than those related to other two temperature intervals.

— The Mn-Al steel with austenitic structure, signed "alloy B" offers a total hydrogen quantity of lower entity compared to those showed by alloy A (Fig. 8). It's possible to notice a trend to a rapid saturation. The trend of the quantities of hydrogen escaped during the different ranges are like those of alloy A.

— The Cr-Ni stainless steel, signed AISI 304 presents more elevated total values of quantities of out-gased hydrogen with a trend absolutely growing, corresponding to the charging time (Fig. 9).

The diagrams related to the quantities of out-gased hydrogen in each ranges present a slope lightly growing according to the first range and approximately constant according to the second range, while the diagram related to the third range is characterized by a more elevated increase of growth.

Discussion

During cathodic charging the permeation and the diffusion coefficient of hydrogen into the steel is heavily influenced, in a complex way, by different matters, not totally explaned in literature: kind and evolution of surface layer, current density, lattice microstructure, presence of traps with different energy.

A review of literature indicates some experiences concerning carbide volume and microstructure effects on hydrogen diffusion in steel [9].

Hydrogen permeability is inversely dependent upon carbon volume fraction and upon carbides fineness.

These dependencies could be explaned considering reversible interface trapping of fine coherent carbides that is associated with blocking of diffusion paths by carbice particles.

According to Johnson and Wu [10] apparent solubility C_{app}, defined by $C_{app} = O(i_c{}^{1/2})/D_{eff}$ [mol H m^{-3}] (where O is the permeability, i_c is the current density during cathodic charging, D_{eff} is the diffusivity), increases with increase in carbon content in annealed steels.

The main differences that characterize the two FeMnAl alloys could be summarized as alfa/gamma interface and carbide in Alloy A with duplex structure and a solid solution with Carbon in interstitial sites of the f.c.c. lattice in Alloy B.

Moreover the apparent diffusivity of hydrogen is $D = D_\alpha D\gamma /(f_\alpha{}^2 D_\gamma + f_\gamma{}^2 D_\alpha)$, where D_α, D_γ are diffusivity of hydrogen in ferrite grain and austenite grain respectively ($D_\alpha = 10^{-11}$ m^2 s^{-1}; $D\gamma = 3 \times 10^{-16}$ m^2 s^{-1}) [10], f_α f_γ are volume fraction, in turn, of ferrite grain and austenite grain [11].

The greatest diffusivity of c.c.c. lattice, in duplex structure permits penetration through the bigger thickness ($x^2 = D$ t) [11].

It's considered that the austenitic Alloy B contains a great quantity of Carbon compared to Alloy A, therefore the austenitic phase of Alloy A has the highest solubility compared to the one of Alloy B.

All this can be valued from the thermal analysis, hence out-gased hydrogen quantity can be correlated with structure apparent solubility, that is bigger in duplex structure.

Conclusions

The analysis of emission diagrams of hydrogen and the graphics of thermal analysis gives the opportunites to make the following considerations:

— The two Mn-Al steels have emission diagrams quite similar; the only difference is the degased hydrogen quantities, that is bigger for the steel signed A, with duplex structure.

There are two emission peaks of low and medium activation energy, under 400 °C and between 400 °C and 600 °C respectively.

— The emission diagrams of AISI 304 steel shows a lower peak of medium energy and a peak between 600 °C and 800 °C, that characterize a strong trap site.

— The alloying of Carbon in solution improves the gamma phase formation and decreases the quantity of out-gased hydrogen, from weak and strong trap sites. This typical behaviour is due to interstitial carbon atoms that can limit the solubility and obstruct the diffusivity of hydrogen crossing the austenitic structure of steel. Therefore, the degased hydrogen quantities from the austenitic steel B seems to have a stationary level with the improvement of cathodic charging time probably just for the presence of Carbon and the austenitic structure.

— The AISI 304 steel shows the bigger quantities of degased hydrogen respect to Mn-Al steels.

References

[1] M. Cavallini, F. Felli, R. Fratesi and F. Veniali, *Aqueous solution corrosion behaviour of "poor man" high manganese-aluminum steels*, Werkstoffe und Korrosion, 33, (1982), 281-284.

[2] G. Bombara, F. Felli and U. Bernabai, *Investigation into the not salt of Cr-Al, Cr-Ni-Mn and Mn-Al steels*, Werkstoffe und Korrosion 33, (1982), 491-497.

[3] U. Bernabai, G.A. Capuano, A. Deng and F. Felli, *High temperature oxidation of Aluminum electroplated Fe-Mn alloys*, Oxidation of Metals, 33 (3/4), (1990), 309-320.

[4] I.F. Tsu and T.P. Perng, *Hydrogen compatibility of FeMnAl Alloys*, Metall Trans. A, 22A, (1991), 215-224.

[5] R.B. Hutchings, A. Turnbull and A.T. May, *Measurement of Hydrogen transport in a duplex stainless steel*, Scripta Metallurgica et Materialia, 25 (1991), 2657-2662.

[6] U. Bernabai, G. Biggiero and R. Torella, *Thermal analysis on hydrogen charged annealed and quenched AISI 420 stainless stell*, to be published on Metallurgical Science and Technology, 11, n. 2 (1993).

[7] J.Y. Lee and S.M. Lee, *Hydrogen trapping phenomena in metals with BCC and FCC crystal structures by the desorption thermal analysis technique*, Surface and Coating Technology, 28 (1986), 301-314.

[8] T. Asaoka *Hydrogen trapping behaviour in plain carbon and Cr-Mo alloy steel*, Proceeding of the MIAMI Interaction Symposium on Metal-Hydrogen System 13-15 April, 1981.

[9] W.M. Robertson and A.W. Thompson, *Permeation measurements of hydrogen trapping in 1045 steel*, Metallurgical Trans. 11A, (1080), 553-557.

[10] D.L. Johson and J.K. Wu, *Hydrogen transport in carbon steels as a function of Carbon content and heat treatment near 298 K*, Materials for Energy Systems, 8, N. 4, (1987), 402-408.

[11] H.E. Tang and N. Chen, *Diffusion of hydrogen in (alfa-gamma) duplex stainless steel*, Acta Metallurgica Sinica, 2, N. 4 (1989), 274-278.

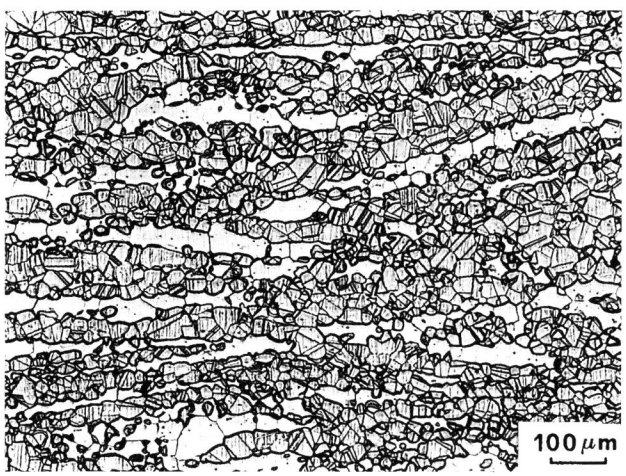

Fig. 1:
Microstructure of Alloy A (44% of alfa phase).

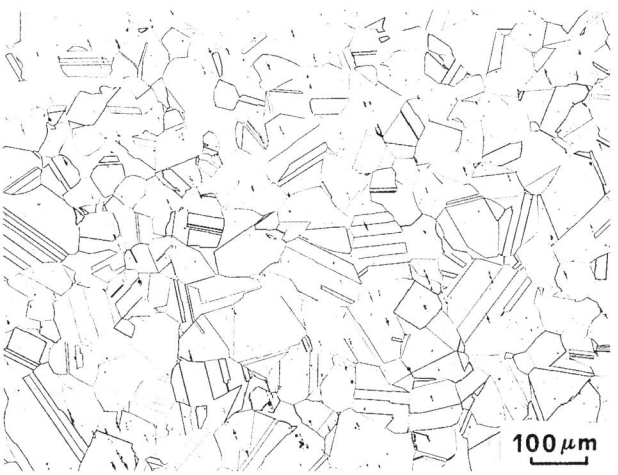

Fig. 2:
Microstructure of Alloy B (0.5% of alfa phase).

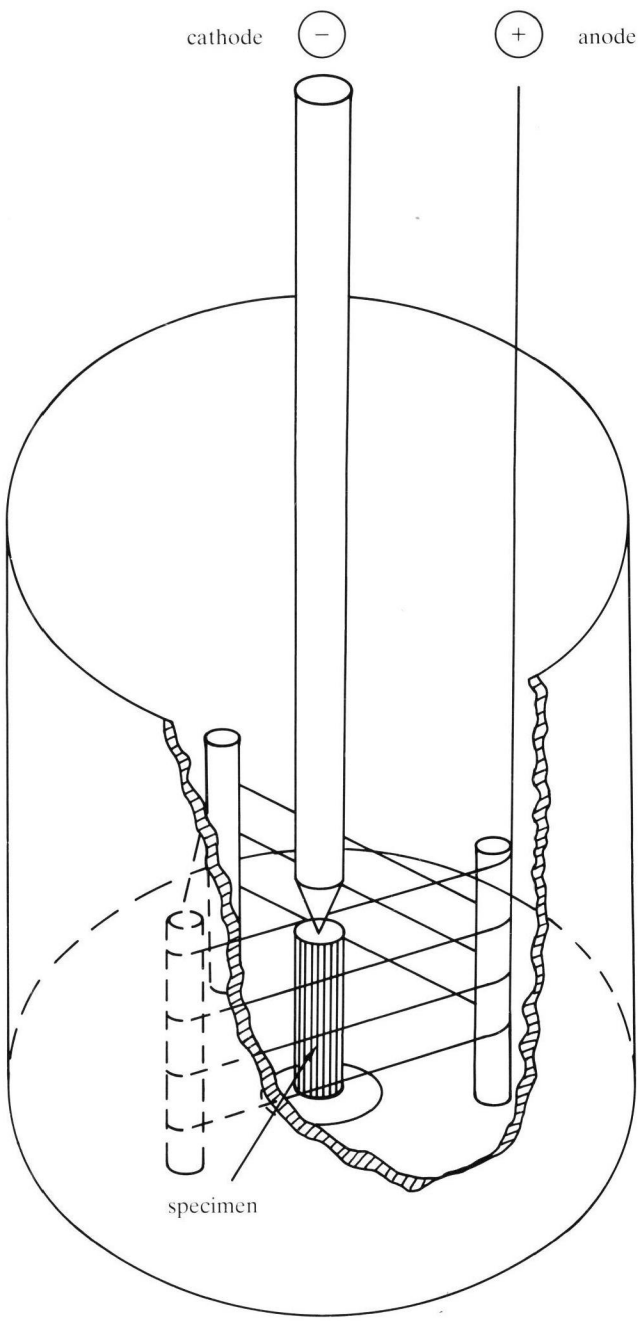

Fig. 3:
Apparatus for cathodic charging of specimen.

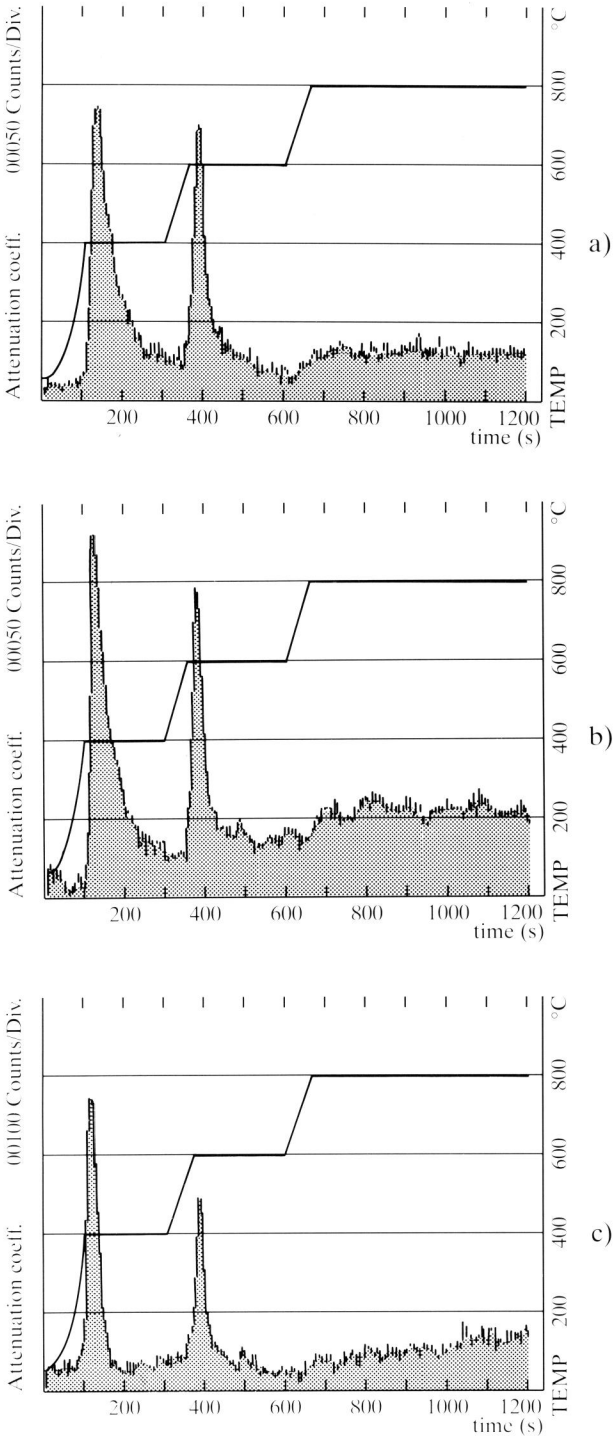

Fig. 4:
Thermal analysis of Alloy A:
a) 100 min of charging
b) 200 min of charging
c) 400 min of charging

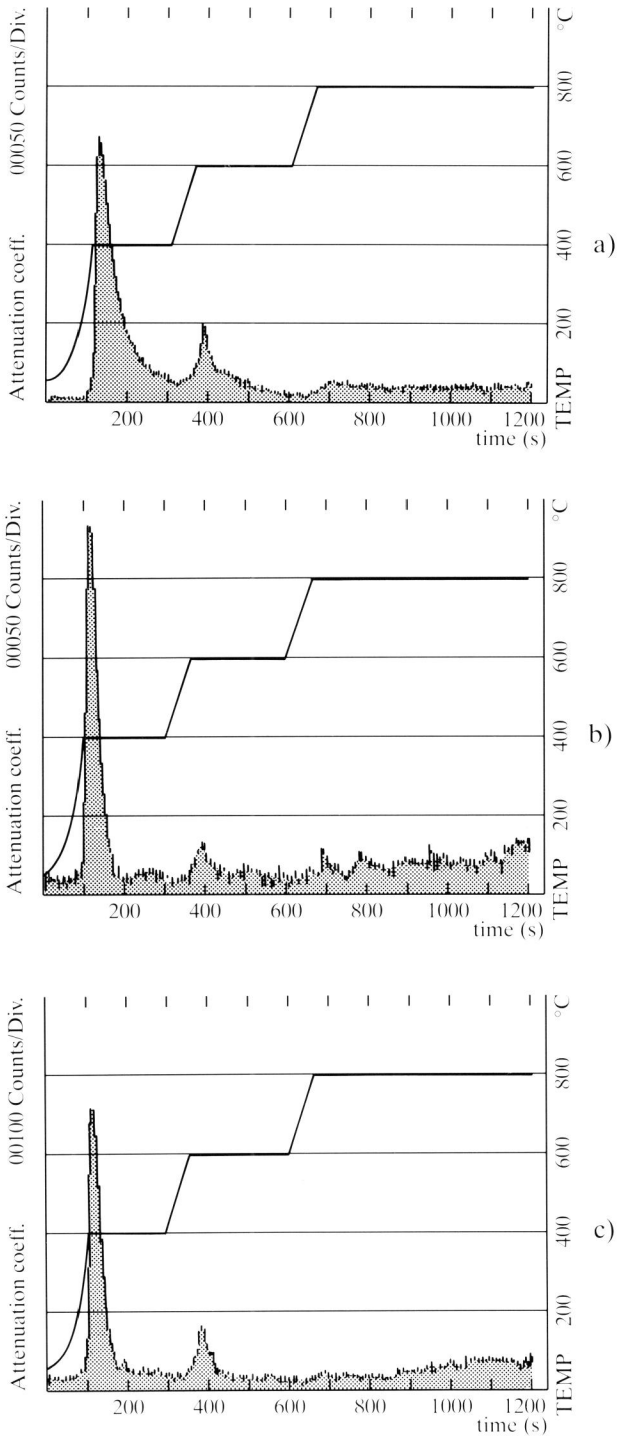

Fig. 5:
Thermal analysis of Alloy B:
a) 100 min of charging
b) 200 min of charging
c) 400 min of charging

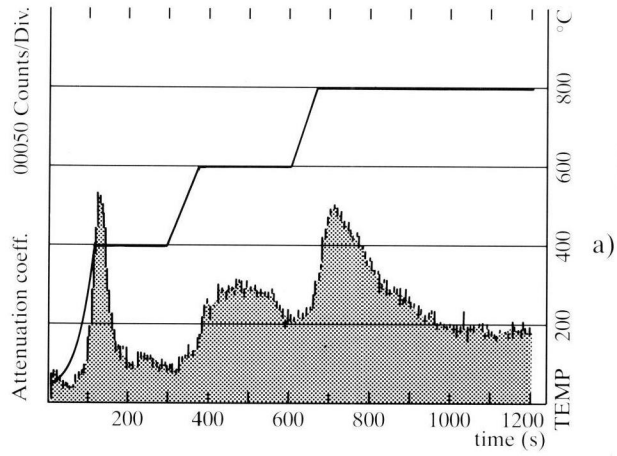

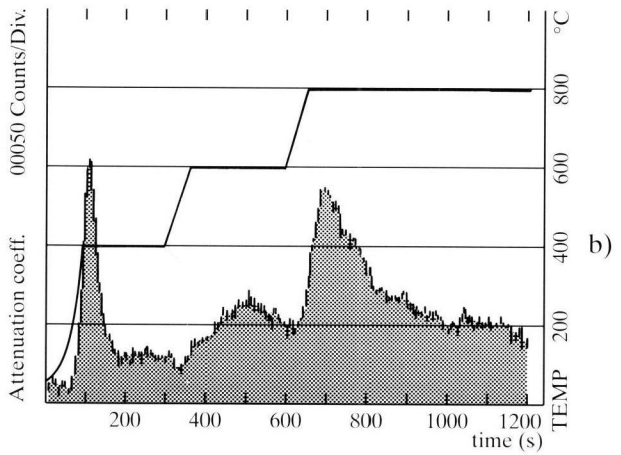

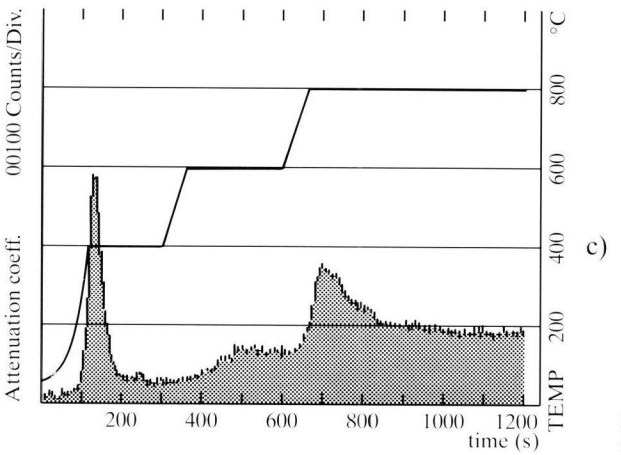

Fig. 6:
Thermal analysis of AISI 304 stainless steel:
a) 100 min of charging
b) 200 min of charging
c) 400 min of charging

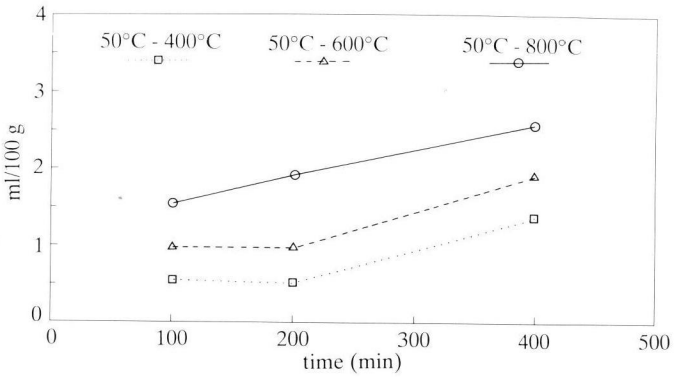

Fig. 7:
Diagrams of degased hydrogen from Alloy A.

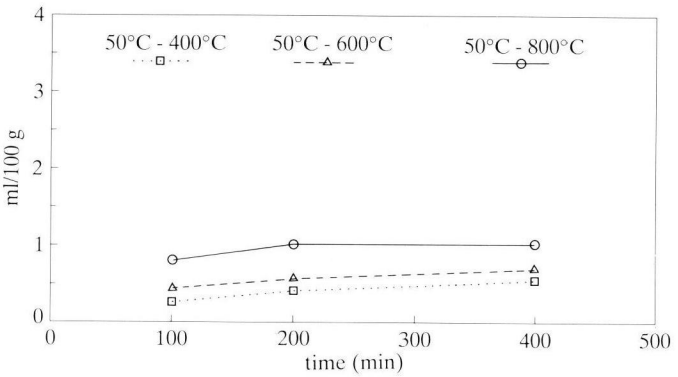

Fig. 8:
Diagrams of degased hydrogen from Alloy B.

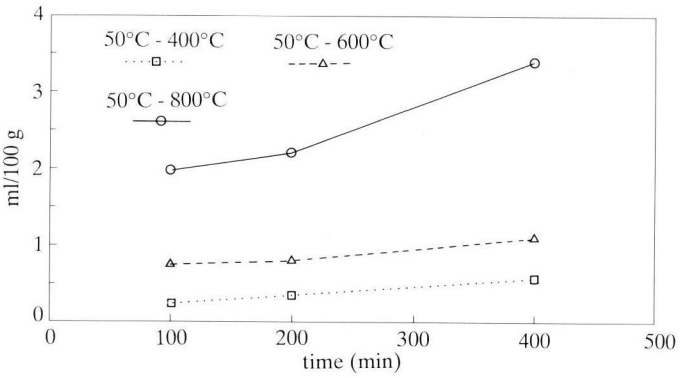

Fig. 9:
Diagrams of degased hydrogen from AISI 304 stainless steel.